Automated Robotic Deburring Using Impedance Control

H. Kazerooni

ABSTRACT: An automated deburring procedure using a robot manipulator is considered for the removal of burrs in the presence of robot oscillations and bounded uncertainties in the tool holder. Electronic compliancy (impedance control) is proposed as an "adaptive" mechanism to satisfy the requirements of this application. The development and implementation of the impedance control methodology on an active end-effector or the whole robot are examined for precision deburring and grinding tasks.

Introduction

Since deburring and grinding are finishing processes, parts at this stage in production have their highest value. Thus, it is essential that deburring be performed economically without producing scrap or the need for rework. This is the motivation for the development of an automated deburring and grinding operation. In most cases, burrs must be removed to allow for the proper fitting of assembled parts and to ensure safe and proper functioning. On high-temperature, high-speed rotating parts, deburring is further required to reduce turbulent gas flow, maintain dynamic balance, and relieve localized stress. For this class of parts, the term "precision deburring" is used. The final geometry of a deburred edge must remain within a given set of tolerances, with a prescribed high-quality finish. Typically, manual deburring is the only method available, which represents a time-consuming and expensive solution. Deburring costs for some cast parts can be as high as 35 percent of the total parts cost. Thus, it is evident that the automation of deburring and grinding operations presents an important opportunity to improve the manufacture of machined parts.

References [1]–[8] contain valuable contributions from previous research. An examination of the work of other researchers reveals that robotic deburring and grinding have generally been studied as a trajectory-following task. Although robotic deburring is a task with final geometrical specifications, the contact forces in the normal and tangential directions are a fundamental part of the process. This suggests that the concept of impedance control should be incorporated into the control scheme. An adaptive system capable of modulating its impedance and integrating the dynamics and uncertainties of the process and the robot is the next logical development. To implement such a control system, an analysis of the nature of the burr is necessary.

Presented at the 1987 Conference on Robotics and Automation, Raleigh, North Carolina, March 31–April 3, 1987. H. Kazerooni is with the Mechanical Engineering Department, University of Minnesota, 111 Church Street, SE, Minneapolis, MN 55455. This research is supported by an NSF grant under Contract NSF/DMC-8604123.

Geometric and Qualitative Model of the Burr

Burrs are formed by many manufacturing processes, and the type of burr formed depends directly on the process used and the prevailing conditions. Burrs can result from the action of cutting tools and tooling imperfections in casting and forming. Although this paper is mainly concerned with the deburring of edges, the results are applicable to other deburring operations as well.

The burr removal tools chosen for our analysis and experiments were rotary files, which produce a 45-deg chamfer on the workpiece edge when the tool is held orthogonal to the part surface. To ensure the complete removal of a given burr, the chamfer width must be larger than the root width, as seen in Fig. 1.

The material removal rate of a deburring pass is a function of the velocity of the tool bit along the edge and the cross-sectional areas of both the chamfer and the burr. This relationship can be expressed as

$$\text{Material removal rate} = (A_{\text{chamfer}} + A_{\text{burr}})\, V_{\text{tool}} \qquad (1)$$

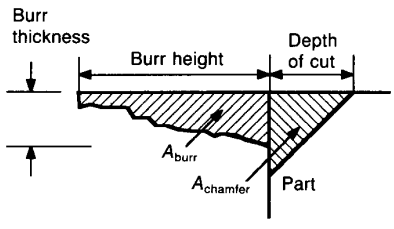

Fig. 1. Typical profile of a burr on a part edge.

The above equation does not reveal any dynamic behavior. It is included to emphasize the proportionality of the material removal rate to feed rate, depth of cut, and chamfer area. Although each of these terms is a function of other variables, such as contact forces and the stiffness of the material, the material removal rate can always be specified with this set of geometric parameters. The exact functional relationship depends, in part, on the control strategy used in the deburring process.

The size and orientation of burrs on a part are completely random in nature. A characterization of the dimensions of edge burrs was generated from burr-height and root-thickness measurements on aircraft engine parts. In that study [9], the height of an average burr was 0.25–0.75 mm (0.010–0.030 in.), with a thickness of 0.025–0.075 mm (0.001–0.003 in.). Burr heights ranged from zero for a sharp corner to 1.5 mm (0.060 in.), and the root thickness from 0 to 0.23 mm (0.009 in.). The ratio $A_{\text{burr}}/A_{\text{chamfer}}$ can vary in a given deburring process from a minimum value of zero for sharp corners, to 0.2 for average burrs, to the worst-case ratio of 2.0, depending on the chamfer area chosen. Therefore, the material removal rate for a given velocity and a desired constant chamfer can vary by as much as a factor of 2.5, depending on the size of the burr.

This large variation in burr dimensions is a key challenge in the design of a control scheme for robotic deburring. Since the force required to cut in the tangential direction is proportional to the material removal rate, it is clear that large variations may be expected in the tangential component of the cutting force.

The cutting force can be resolved into two vector components: the tangential force exerted in the direction of tool movement and the normal force exerted perpendicular to the workpiece surface. The cutting force is largely a function of the average surface area of the cut for a given feed rate [Eq. (1)]. The projected areas, as seen in the model, are simply geometric functions of the intersection between the part corner, the burr, and the milling cone. As such, variations in the burr size should not greatly affect the normal force for a given chamfer (Fig. 2). To summarize the findings of this section: (1) For a

0272-1708/88/0200-0021 $01.00 © 1988 IEEE

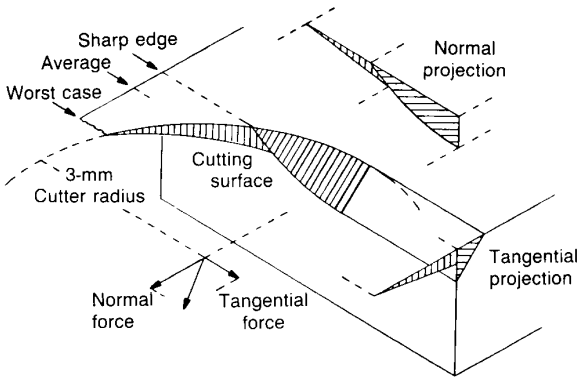

Fig. 2. Cutting surface area, 45-deg conic mill.

given constant feed rate, the tangential force varies significantly with variation of the burr size; in other words, every time the rotary file encounters a large burr, the tangential force increases dramatically. (2) For a given constant feed rate, the normal force stays relatively constant regardless of burr-size variation. These results were experimentally confirmed, as discussed in the last section.

The preceding findings have been verified in practice, as they cause difficulties in most control schemes for robotic deburring. When the cutting tool is moved with constant speed along the edge by an industrial robot, the tangential force imposed on the end point varies significantly due to the variation of the burr size. If the burr is large enough, the contact force increases until a separation of the tool piece from the part occurs. We seek to develop a self-tuning strategy such that the contact force in the cutting process is minimized. A small contact force would guarantee that the end point of the robot could follow the part without separation.

Strategy for Robotic Deburring

Consider the deburring of a surface by a robot manipulator; the objective is to use an end-effector to smooth the surface down to the commanded trajectory, depicted by the dashed line in Fig. 3. Following the preceding discussion, our goal is to design a control

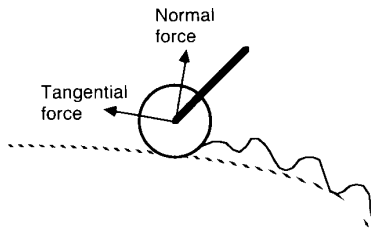

Fig. 3. Deburring an edge.

mechanism for the manipulator with a large impedance (small compliance) in the normal direction and a small impedance (large compliance) in the tangential direction. *Impedance* is defined as the ratio of the contact force to the end-effector deflection as a function of frequency. A large impedance in the normal direction causes the end point of the tool bit to resist the interaction forces and stay very close to the commanded trajectory (dashed line). The larger the impedance of the end-effector in the normal direction, the smoother the surface will be. Once the volume of metal to be removed is known, the desired tolerance prescribes an approximate value for the impedance in the normal direction.

As described, the force necessary to cut in the tangential direction at a constant traverse speed is approximately proportional to the volume of metal to be removed [10]. Therefore, when the cutting tool encounters a large burr, the contact force increases and the manipulator must decrease the tangential component of its speed to maintain a constant tangential force. This will result in a smaller volume of metal to be removed per unit of time, and, consequently, less force in the tangential direction.

The preceding explanation demonstrates that it is necessary for the end-effector to accommodate the interaction forces along the tangential direction, which directly implies a small impedance value in the tangential direction. A small value for the tangential impedance relative to the normal impedance guarantees small contact forces in the tangential direction. If a designer does not accommodate the interaction forces by specifying a small stiffness value in the tangential direction, the cutting tool may stall or break, or a slight deflection may develop in the end-point position in the normal direction. Either of these events is likely to result in a cut that exceeds the desired tolerance.

The frequency spectrum of the roughness of the surface and the desired translational speed of the robot along the surface determine the *frequency range of operation*, ω_b. ω_b is the frequency range of the burr seen from the end-effector. The following equalities summarize the dynamic characteristics required for deburring with a robot without positioning uncertainties, where δX_n and δX_t are the end-point deflections normal and tangential to the part, and δF_n and δF_t are the normal and tangential contact forces.

$$|\delta X_n(j\omega)/\delta F_n(j\omega)| \triangleq \text{very small for all } \omega \text{ belonging to } \omega_b \tag{2}$$

$$|\delta X_t(j\omega)/\delta F_t(j\omega)| \triangleq \text{very large for all } \omega \text{ belonging to } \omega_b \tag{3}$$

This analysis is correct when there are no positional uncertainties in the robot end-point position. An examination of the performance characteristics of one such industrial robot illustrates the difficulties that can arise. The General Electric P50 has a limited programmable resolution of 0.25 mm (0.01 in.). Furthermore, the robot end-point position at a programmed point is characterized by a low-frequency periodic motion with a peak-to-peak amplitude of 0.1 to 0.2 mm. Even without considering the fixturing uncertainties, these positional uncertainties are about 0.35 mm. Thus, the P50 by itself is unsuitable for precision deburring tasks. We assume that the robot vibration and the positional uncertainties occur at the bounded frequency range of ω_r.

One common solution to this problem is to add a compliant end-effector such that $|\delta X_n(j\omega)/\delta F_n(j\omega)|$ is large for all $0 < \omega < \omega_r$ to compensate for the uncertainties in the robot position. However, this solution results in a dilemma for the designer. To compensate for low-frequency uncertainties in robot position, a large normal compliance (small impedance) in the end-effector is needed, while a small compliance (large impedance) is required for deburring purposes.

An end-effector with the dynamic characteristics shown in Fig. 4 would satisfy both requirements. As shown in Fig. 4, $|\delta X_n(j\omega)/\delta F_n(j\omega)|$ is very large for all $\omega \in \omega_r$ and very small for all $\omega \in \omega_b$. While a large $|\delta X_n(j\omega)/\delta F_n(j\omega)|$ in $(0, \omega_r)$ does not let the robot oscillations develop a large variation in the normal contact force, a small $|\delta X_n(j\omega)/\delta F_n(j\omega)|$ in ω_b will cause the end-effector to be very stiff in response to the

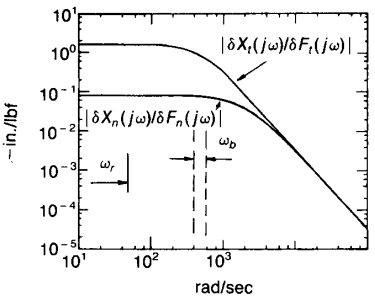

Fig. 4. Ideal dynamic behavior for the end-effector.

burrs. The following is a summary of the desired characteristics of the end-effector in the normal direction.

- $|\delta X_n(j\omega)/\delta F_n(j\omega)|$ must be large for all ω belonging to ω_r
- $|\delta X_n(j\omega)/\delta F_n(j\omega)|$ must be small for all ω belonging to ω_b

But it is impossible to design and build a passive end-effector [using a Remote Center Compliance (RCC)] with the dynamic behavior illustrated in Fig. 4 [9]. An examination of the equations for the normal and tangential motion of a passive end-effector reveals that a constant mass of the tool appears in both dynamic equations (tangential and normal directions) of the passive end-effector. Thus, for a given set of RCC constants, one cannot choose arbitrary natural frequencies (approximately bandwidths) in both directions. References [11] and [12] describe the applications of some passive end-effectors. Impedance control [13]–[18] is the only method able to develop electronically the dynamic behavior given in Fig. 4. The impedance control method guarantees that the different stiffnesses required for the tangential and normal directions will be achieved for a system over a bounded frequency range. Thus, we see that the design goals and the resulting dilemma lead us to consider the implementation of impedance control.

Electronic Compliancy; Impedance Control

A complete description of the control method to develop electronic compliancy (impedance control) for a multidegree-of-freedom nonlinear manipulative system is given in [17] and [18]. For our purposes, however, it is sufficient to frame the controller design objectives for a deburring operation by a set of meaningful mathematical terms; followed by a summary of the controller design method to develop compliancy.

The controller design objective is to provide a stabilizing dynamic compensator for the system such that the ratio of the position of the end point of the end-effector to an interaction force is constant within a given operating frequency range. This statement is expressed mathematically in Eq. (4), where $\delta F(j\omega)$ is the 2×1 vector of the deviation of the interaction forces from their equilibrium value in the global Cartesian coordinate frame, $\delta X(j\omega)$ is the 2×1 vector of the deviation of the end-point position from the nominal point in the global Cartesian coordinate frame, K is the $2 \cdot \times 2$ real-valued, nonsingular diagonal stiffness matrix with constant members, ω_0 is the bandwidth (frequency range of operation), and j is the complex number notation, $\sqrt{-1}$.

$$\delta F(j\omega) = K\,\delta X(j\omega) \quad \text{for all } 0 < \omega < \omega_0 \qquad (4)$$

Since the deburring process has been framed as a two-dimensional process, all vectors in Eq. (4) are of two dimensions. The stiffness matrix K is specified by the designer, depending on the application, to govern the behavior of the end-effector in constrained maneuvers. Large elements of the K matrix imply large interaction forces and torques for a given displacement. Small members of the K matrix allow for a considerable amount of motion in the end-effector in response to interaction forces. Although a diagonal stiffness matrix is appealing for the purpose of static uncoupling, the K matrix generally is not restricted to any structure.

The frequency range of operation, ω_0, is also an important parameter that must be considered by the designer. Mechanical systems are not generally responsive to external forces at high frequencies greater than the bandwidth of their controller [19], [20]. As the frequency increases, the effect of the feedback disappears gradually (depending on the type of controller used), until the inertia of the system dominates the overall motion. Therefore, depending on the dynamics of the system, Eq. (4) may not hold for a wide frequency range.

In summary, Eq. (4) defines K, which is the relationship between $\delta F(j\omega)$ and $\delta X(j\omega)$, valid for a bounded range of ω_0. In addition to choosing an appropriate stiffness matrix, K, and a viable ω_0, a designer must also guarantee the stability of the closed-loop system. The goal is to obtain dynamic behavior for the manipulative system that resembles that shown in Fig. 4.

Figure 5 illustrates the architecture of the closed-loop control system for the end-effector. The detailed description of each operator in Fig. 5 is given in [17] and [18]. Since the dynamic behavior of the end-effector in the neighborhood of its operating point is linear, all of the operators in Fig. 5 are considered to be transfer-function matrices. However, in the general approach for development of compliancy [17], [18], E, G, H, and S are nonlinear operators.

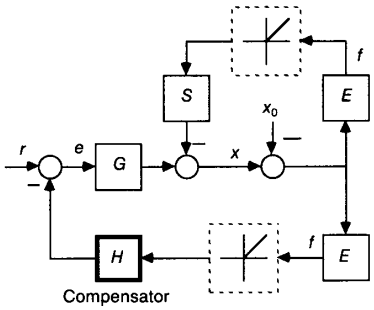

Fig. 5. Closed-loop control for the end-effector.

The transfer-function matrix G represents the dynamic behavior of the end-effector with a positioning controller. The input to G is an $n \times 1$ vector of the input trajectory, e. The fact that most manipulative systems have some kind of positioning controller is the motivation behind our approach. Many methodologies are available for the development of robust positioning controllers. G can be calculated experimentally or analytically. Note that G is approximately equal to the unity matrix for the frequencies within its bandwidth.

The sensitivity transfer-function matrix S represents the relationship between the external force on the end point of the end-effector and the end-point motion. This motion is due to compliance from the end-effector mechanism and the positioning controller. To obtain good positioning, S must be quite "small." The notion of "small" can be regarded in the singular-value sense when S is a transfer-function matrix. L_p-norm [17], [18] can be considered to show the size of S in the nonlinear case.

The dynamic behavior of the environment is given by E and, in general, is a nonlinear mapping. A simple model of the environment can be represented by a spring, where E represents the stiffness of the spring.

The compensator to be designed is given by H. The input to this compensator is the contact force. The compensator output signal is subtracted from the input command vector r to give the error signal e as the input trajectory for the robot manipulator. The

value of the contact force and the end-point position of the robot are given by

$$f = E(I + SE + GHE)^{-1}Gr \qquad (5)$$

and

$$y = (I + SE + GHE)^{-1}Gr \qquad (6)$$

The general goal is to choose a class of compensators, H, to shape the impedance of the system $E(I + SE + GHE)^{-1}G$ in Eq. (5). When the system is not in contact with the environment, the actual position of the end point is equal to the input trajectory command within the bandwidth of G. As noted earlier, G is approximately equal to the unity matrix within its bandwidth. When the system is in contact with the environment, then the contact force follows r according to Eq. (5). The input command vector r is used differently depending on whether the tool piece is in contact with the workpiece or traveling through unconstrained space. When the manipulative system and environment are in contact, r is a command to shape the contact force. It is a trajectory command when it seeks to move the manipulator in unconstrained space.

In impedance control, we do not command any set point for force as in admittance control [21], [22]. This method is called *impedance control* because it accepts a position vector as input and reflects a force vector as output. There is no hardware or software switch in the control system when the robot travels from unconstrained space to constrained space—in our case, when the grinder encounters the workpiece. The feedback loop on the contact force closes naturally when the robot encounters the environment (workpiece). When the system is in contact with the environment, then the contact force is a function of r according to Eq. (5). This compensator must also guarantee the stability of the system.

We are interested in a particular case when $r = 0$. Suppose the environment is moved into the end-effector or the end-effector is moved into the environment. In the case of robotic deburring, the end point of the robotic manipulator is then in contact with a very stiff environment. When the environment is very stiff, E approaches ∞ in the singular-value sense, and the relationship between the contact force and the end-point deflection is given by Eq. (7) [17].

$$f = (S + H)^{-1}x \qquad (7)$$

Equality (7) is derived by inspection of the block diagram in Fig. 5. The role of $(S + H)^{-1}$ is analogous to the stiffness matrix K defined by Eq. (4). With S known, one can select appropriate and stabilizing values of H such that $(S + H)^{-1}$ of Eq. (7) will meet the deburring requirements as given by Eq. (4). According to Eq. (7), the gain H adds to the existing passive compliance in the system. If there is enough passive compliance in the system for a particular task (for example, a RCC is mounted on the robot wrist), then there is no need for extra compliance via feedback gain H.

Experimental Setup

An experiment was conducted to verify the feasibility of using impedance control in robotic deburring. The principal purpose of this experiment was to investigate whether this control methodology could reliably perform the deburring task to the preceding specifications in the absence of position uncertainties such as robot oscillation. Experiments to validate the use of impedance control to correct for robot position uncertainties will be completed as a second phase of this series of experiments. A fast, high-precision XY table for planar maneuvering was used to eliminate robot oscillation and reaction forces. Figure 6 shows the experimental setup.

The workpiece to be deburred was mounted on the XY table for maneuvering while the grinder was held vertically by a stationary platform. The sample part was mounted on the table with a sample holder. Depending on the geometry of the part, various holders could be made. Figure 7 shows that the sample holder used to hold a rectangular part. Of course, in the actual deburring process, it may be better to move the grinder with the robot while the part is on a stationary platform. Our scheme was chosen to eliminate undesired robot oscillations and other positional uncertainties.

Reference [23] describes an active end-effector that can be held by commercial robot manipulators. One can develop electronic compliancy for this active end-effector. Our experimental setup was designed primarily to understand the nature of forces in the cutting mechanics under the influence of an impedance control scheme. The XY table was interfaced to a microcomputer for control. Two force sensors between the part and the XY table platform allowed for measurement of the interaction forces between the part and the grinder. The sampling time of the control algorithm is 4 ms.

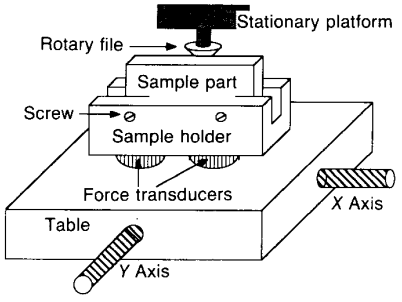

Fig. 6. Experimental setup.

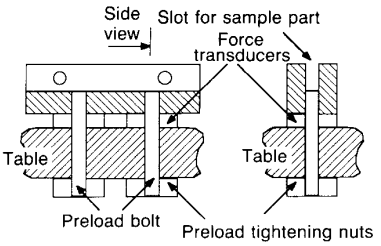

Fig. 7. Fixture to hold the straight-edge sample part.

The objective of this experiment was to compare the size of the cutting forces when impedance control is used to control the XY table with the case when only velocity control is used along the tangential direction. The parts to be deburred were rectangular aluminum $2 \times 5 \times 0.25$ in., as shown in Fig. 8.

The edge of the sample part was filed to produce step burrs as shown in Fig. 8. The depth of cut was 0.06 in. The XY table was commanded to move in the X direction to encounter the burr with a constant feed rate of 0.036 in./sec. Figure 9 shows the tangential and normal forces when no impedance control is employed in the tangential direction. As seen in Fig. 9, once the grinder encountered the burr, the tangential force increased to 25 newtons (nt) and the deburring tool stalled. The feed rate was constant and the tangential force increased proportionally to the material removal rate as expected. From the results in Fig. 9, it is intuitive to develop a system that slows the XY table when the grinder encounters the burr.

In the next set of experiments, impedance control was employed to govern the XY table motion. A large and a small impedance were

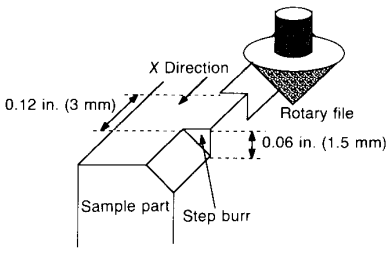

Fig. 8. Sample part with step burr.

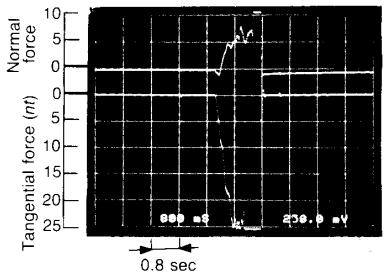

Fig. 9. Tangential and normal forces in the deburring process with constant feed rate of 0.036 in./sec.

specified in the normal and tangential directions of the part, respectively. Note that these impedance values were chosen to satisfy the stability condition given in [17] and [18]. One can choose a variety of impedances. The choice of impedance is a function of the variables, such as feed rate, depth of cut, and the metal stiffness. Figure 10 shows the normal and tangential forces. When the grinder encountered the burr, the control system slowed the table to grind the burr. It took about 5 × 0.8 sec to remove the burr. The average tangential force did not increase as much as in the previous experiment because the tangential impedance of the table was chosen to be small. The oscillation of the contact force is due to the contribution of the inertia of the sample holder and the sample part in the measurements of the contact forces. This suggests the installation of the force sensors in the stationary part of the system.

Conclusion

An automated deburring procedure using a robot manipulator was considered for the removal of burrs in the presence of robot oscillations and bounded uncertainties in the location of the robot end point relative to the part. To remove the burr, high and low impedances were required in the tool holder in the normal and tangential directions, respectively, for the frequency range that burrs are seen by the robot. To compensate for robot oscillations and positional uncertainties, a low impedance in the normal direction was required for the end-effector for the frequency range of the robot oscillations. The preceding two requirements for deburring and oscillation compensation established the design rules for a deburring control strategy. A passive system could not satisfy the two design rules because of the role the constant mass of the grinder plays in the dynamic behavior of the end-effector. Therefore, impedance control was chosen to satisfy the design rules for robotic deburring and grinding. This paper examined the development and implementation of impedance control methodology for precision deburring. Some of the theoretical results have been verified experimentally, and a second phase of experiments is planned to include the full effects of robot oscillations and workpiece position uncertainties.

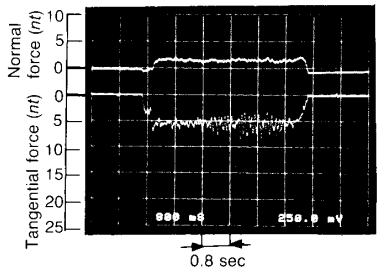

Fig. 10. Tangential and normal forces in deburring with impedance control.

References

[1] E. Abele, D. Boley, and W. Sturz, "Interactive Programming of Industrial Robots for Deburring," *Proc. 14th Int. Industrial Robot Symp.*, Oct. 1984.

[2] T. Bopp, "Robotic Finishings Applications: Polishing, Sanding, Grinding," *Proc. 13th Int. Industrial Robot Symp.*, 1983.

[3] L. Gustaffson, "Deburring with an Industrial Robot," Technical Report, Society of Manufacturing Engineers, 1983.

[4] A. Mortenson, "Automatic Grinding," *Proc. 13th Int. Industrial Robot Symp.*, Aug. 1983.

[5] D. Seltzer, "Tactile Sensory Feedback for Difficult Robot Tasks," *Proc. Robots VI Conf.*, Detroit, MI, Mar. 1982.

[6] R. Thenander, "Practical Examples of Deburring with ASEA Robot," *Proc. 6th Ann. British Robot Assoc. Conf.*, 1983.

[7] H. J. Warnecke, M. Schewizer, and E. Abele, "Cleaning of Castings with Sensor Controlled Industrial Robots," *Proc. 10th Industrial Robot Symp.*, 1980.

[8] D. J. Williams and R. G. Phillips, "Robotic Deburring of Connecting Rod Liner Slots," *Proc. 7th Ann. British Robot. Assoc. Conf.*, 1984.

[9] H. Kazerooni, J. J. Bausch, and B. M. Kramer, "Automated Deburring by Robot Manipulators," *ASME J. Dyn. Syst., Meas., Contr.*, Dec. 1986.

[10] N. H. Cook, *Manufacturing Analysis*, Reading, MA: Addison-Wesley, 1966.

[11] H. Asada and N. Goldfine, "Optimal Compliance Design for Grinding Robot Tool Holders," IEEE Int. Conf. Robotics and Automation, 1985.

[12] J. J. Bausch, B. M. Kramer, and H. Kazerooni, "Compliant Tool Holders for Robotic Deburring," ASME Winter Annual Meeting, Dec. 1986.

[13] N. Hogan, "Impedance Control: An Approach to Manipulation; Part 1: Theory; Part 2: Implementation; Part 3: Applications," *ASME J. Dyn. Syst., Meas., Contr.*, pp. 1–23, Mar. 1985.

[14] N. Hogan, "Impedance Control of Industrial Robots," *J. Robotics and Computer Integrated Manufacturing*, vol. 1, no. 1, pp. 97–113, 1984.

[15] H. Kazerooni, T. B. Sheridan, and P. K. Houpt, "Fundamentals of Robust Compliant Motion for Robot Manipulators," *IEEE J. Robotics and Automation*, vol. 2, no. 2, June 1986.

[16] H. Kazerooni, P. K. Houpt, and T. B. Sheridan, "A Design Method for Robust Compliant Motion for Manipulators," *IEEE J. Robotics and Automation*, vol. 2, no. 2, June 1986.

[17] H. Kazerooni, "Robust Nonlinear Impedance Control for Robot Manipulators," IEEE Conference on Robotics and Automation, Raleigh, NC, April 1987.

[18] H. Kazerooni, J. Guo, and J. Baikovicius, "Compliant Motion Control for Robot Manipulators, Input-Output Approach," American Control Conference, Minneapolis, MN, June 1987.

[19] H. Kazerooni and P. K. Houpt, "On the Loop Transfer Recovery," *Int. J. Contr.*, vol. 43, no. 3, Mar. 1986.

[20] H. Kazerooni, P. K. Houpt and T. B. Sheridan, "An Approach to Loop Transfer Recovery Using Eigenstructure Assignment," *Amer. Contr. Conf.*, Boston, MA, pp. 796–803, June 1985.

[21] M. H. Railbert and J. Craig, "Hybrid Position/Force Control of Manipulators," *ASME J. Dyn. Syst., Meas., Contr.*, June 1981.

[22] D. E. Whitney, "Force-Feedback Control of Manipulator Fine Motions," *ASME J. Dyn. Syst., Meas., Contr.*, June 1977.

[23] H. Kazerooni and J. Guo, "Direct Drive Active Compliant End-effector; Active RCC," IEEE Conf. Robotics and Automation, Raleigh, NC, Apr. 1987.

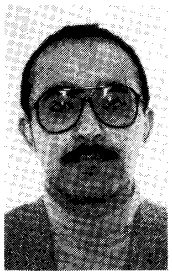

H. Kazerooni was born in Tehran, Iran, in May 1956. He received the M.S. degree in mechanical engineering from the University of Wisconsin, Madison, in 1980, and the M.S.M.E. and Sc.D. degrees in mechanical engineering from the Man-Machine Systems Laboratory of the Massachusetts Institute of Technology, Cambridge, in 1982 and 1984, respectively. From 1984 to 1985, he was with the Laboratory of Manufacturing and Productivity of the Massachusetts Institute of Technology as a Postdoctoral Fellow. He is currently Assistant Professor in the Mechanical Engineering Department at the University of Minnesota, Minneapolis.